Quenching of Tryptophan Phosphorescence in *Escherichia coli* Alkaline Phosphatase by Long-Range Transfer Mechanisms to External Agents in the Rapid-Diffusion Limit†

Joseph V. Mersol,‡ Duncan G. Steel,‡ and Ari Gafni*,§

Institute of Gerontology and Departments of Physics, Electrical Engineering, and Biological Chemistry, University of Michigan, Ann Arbor, Michigan 48109

Received June 7, 1990; Revised Manuscript Received October 2, 1990

ABSTRACT: Quenching of the room-temperature phosphorescence of *Escherichia coli* alkaline phosphatase by several freely diffusing molecules was studied, each of whose absorption spectrum overlaps the long-lived emission of this protein and which therefore can quench the excited triplet state by diffusion-enhanced Förster energy transfer. The presence of additional nonresonance transfer mechanisms was also detected, from a lack of linear dependence of quenching rate on spectral overlap. The quenching agents used were the dye molecules methyl red, methyl orange, and 2-[(4-hydroxyphenyl)azo]benzoic acid, as well as the embedded heme groups of myoglobin, metmyoglobin, and the reduced and oxidized forms of cytochrome *c*. Quenching was found to be greatly diminished upon reduction of each acceptor, indicating that electron transfer occurs efficiently from the excited tryptophan to the oxidized form of the acceptors. The elimination of this electron transfer in the reduced form affords the opportunity to separately measure the Förster transfer rates for the heme proteins. When the transfer rate constant thus measured for myoglobin is applied to a model where both donor and acceptor proteins are taken to be spherical with both tryptophan and the heme group placed off center (a model whose quenching rate equation is newly presented here), the depth of the phosphorescent tryptophan beneath the surface of alkaline phosphatase is found to be 16 Å. This value is close to the depth of tryptophan 109 (which is known to be the phosphorescent residue in alkaline phosphatase), showing that with properly chosen probes this technique is indeed valuable for distance determinations in protein structure studies. The distance calculated from cytochrome *c* data was found to vary among different buffers and also to depend on buffer concentration, changing from 8 to 12 Å upon increase of Tris·HCl concentration from 50 mM to 1 M. This reflects the need for a model for cytochrome *c* which better represents its shape and electrostatic properties.

Fluorescence quenching is an established and useful spectroscopic tool for the study of protein structure in solution. However, the short decay time of fluorescence usually limits the applicability of this approach to rapid quenching since the latter process must compete with fluorescence. Recently, tryptophan residues in a large number of proteins have been found to emit room-temperature phosphorescence provided that molecular oxygen is extensively removed (Saviotti & Galley, 1974; Vanderkooi et al., 1987; Papp & Vanderkooi, 1989). The long decay time of this phosphorescence (milliseconds to seconds) allows the study of interactions that occur on this extended time scale through their effects on the phosphorescence decay kinetics. Of particular interest are long-range interactions since these allow the study of tryptophan residues which are buried inside the protein—residues which, as a rule, are responsible for most proteins' phosphorescence (Kai & Imakubo, 1979; Strambini & Gonnelli, 1985). These interactions also enable one to use quenchers which are free in solution and not bound to the protein, thereby minimizing their effects on the protein's intrinsic structure and making protein labeling (sometimes a tedious task) unnecessary. To ensure that the quenching was by long-range interactions, the quenchers used in this study were all large enough to make direct collision with the excited tryptophan residue in the studied enzyme insignificant (Calhoun et al., 1988).

Three long-range mechanisms which are capable of quenching Trp[1] phosphorescence are energy exchange interactions, electron transfer, and dipole–dipole nonradiative energy transfer. The relative strength of these interactions varies widely with distance and chemical environment. The rate constant $k^{ex}(r)$ for quenching by exchange interactions has been shown by Dexter (1953) to decline exponentially with the distance separating the donor–acceptor pair, having the general form $k^{ex}(r) = k_0^{ex}e^{-2r/L}$ for a given separation r. k_0^{ex} is the quenching rate constant at the van der Waals contact distance between the donor–acceptor pair, r is the distance above the van der Waals contact separating the two, and L is an effective Bohr radius (~0.8–1 Å typically). The rapid decline of k^{ex} with distance separating donor and acceptor (by a factor of ~10 per angstrom) makes exchange interactions relatively short range. Indeed, Stryer has shown that the contribution of these interactions to the quenching of a Tb^{3+} chelate by a Co^{3+} chelate becomes negligible above about 13

† This research was supported by a Presidential Initiative Fund award to the University of Michigan from the W. K. Kellogg Foundation and by a grant from the Office of Naval Research. In addition, the YAG laser was supplied by Spectra-Physics in a joint collaboration to develop laser-based spectroscopy methods. J.V.M. was supported by a training grant from the National Institute on Aging (Contract T32AG00114).

* To whom correspondence should be addressed.

‡ Institute of Gerontology and Departments of Physics and Electrical Engineering.

§ Institute of Gerontology and Department of Biological Chemistry.

[1] Abbreviations: AP, alkaline phosphatase; Mb, myoglobin; met-Mb, metmyoglobin; MR, methyl red; MO, methyl orange; HABA, 2-[(4-hydroxyphenyl)azo]benzoic acid; Trp, tryptophan.

0006-2960/91/0430-668$02.50/0

Å (Stryer, 1982) while Li et al. (1989) estimated the effective range for quenching of the Trp triplet state by disulfide groups at about 8 Å.

The rate constant of electron transfer also shows an exponential decay with distance (in the asymptotic limit of large r), of the form $k^{el}(r) = k_0^{el}e^{-2r/L}$ (Mayo et al., 1986). The effective distance L for electron transfer, however, strongly depends on the medium separating donor and acceptor, with typical values ranging from 0.5 to 2.0 Å. Thus, electron transfer among groups embedded in the interiors of different proteins may occur rapidly over distances of as much as 15–20 Å (Marcus & Sutin, 1985) and probably involves regions with increased electron conductivity in these molecules. Electron transfer also depends on the redox potential of the donor–acceptor pair and may be modulated by changing the oxidation state of the acceptor. In this work we exploit this property to determine the relative contributions of electron transfer and resonance energy transfer to the quenching of AP phosphorescence.

The theory of singlet–singlet resonance energy transfer by dipole–dipole interactions was developed by Förster (1948), and the rate constant of transfer by this mechanism is given by

$$k_t = k_0(R_0/r)^6 \quad (1)$$

where k_0 is the rate constant for the decay of the excited state of the donor in the absence of the acceptor, r is the distance separating the donor–acceptor pair, and R_0 is the distance between donor and acceptor at which the efficiency of transfer is 50%. This term is given by $R_0 = (9.79 \times 10^3)(Q_0K^2Jn^{-4})^{1/6}$, where Q_0 is the quantum yield of the donor in the absence of acceptor, n is the refractive index of the medium, and K, the orientational factor, is given by the expression $K = \cos \alpha_{DA} - 3 \cos \alpha_D \cos \alpha_A$, where α_{DA} is the angle between donor and acceptor dipoles and α_A and α_D are the angles defined by the donor and acceptor dipoles, respectively, and the line joining them. J, the spectral overlap integral, is given by the equation $J = \int f(\nu)\epsilon(\nu)\nu^{-4}\, d\nu / \int f(\nu)\, d\nu$, where $f(\nu)$ and $\epsilon(\nu)$ are the luminescence intensity of the donor and the extinction coefficient of the acceptor, respectively, at wavenumber ν. In the case of triplet–singlet transfer, the quantum yield Q_0 is replaced by ϕ_p, the radiative efficiency of the triplet state (Galley & Stryer, 1969).

Many of the past studies employed resonance energy transfer to determine the distance between pairs of donors and acceptors whose relative movement, during the lifetime of the excited state of the donor, was insignificant [for a review, see Stryer (1978)]. This static limit is typical of many fluorescent chromophores linked to large, rigid, macromolecules like proteins where changes in the distance between donor and acceptor binding sites are minimal on the nanosecond time scale typical of fluorescence decay. The theory of energy transfer at the static limit was further developed by Förster to include the case where each donor is surrounded by an ensemble of randomly distributed acceptors (Förster, 1949). As expected, while each individual donor decays exponentially, the emission from the ensemble of donors as a whole decays nonexponentially. This work was extended by several groups (Gösele, 1978; Klein et al., 1976; Gösele et al., 1975; Millar et al., 1981) to consider the enhancement of energy transfer rate by weak diffusion. Effects of diffusion on the energy transfer process and its rate have also been evaluated by Steinberg and Katchalski (1968) and by Steinberg et al. (1983) and applied to study the conformation and dynamics of oligopeptides by determination of the rates of translational Brownian motion of the ends of these molecules.

The enhancement of energy transfer by diffusion is maximal in the limit where the mean combined distance traversed by donor and acceptor during the excited-state lifetime of the former is much greater than the average distance separating them (Thomas et al., 1978). This rapid-diffusion limit is reached when $6D\tau_0 \gg S^2$, where D is the sum of the diffusion coefficients of the donor and acceptor, τ_0 is the donor's lifetime in the absence of acceptor, and S is the mean distance between donor and acceptor. Under these conditions the time-averaged distribution of acceptors around a given donor becomes homogeneous, and the rate for Förster energy transfer was shown (Thomas et al., 1978; Stryer et al., 1982) to allow for the determination of the distance of closest approach between donor and acceptor. In the simple case where the donor and acceptor chromophores are in the centers of spheres, the transfer rate is given by

$$k_t = \frac{4\pi}{3}\rho_A k_0 R_0^6/a^3 \quad (2)$$

where a is the distance of closest approach (the sum of the radii of the donor and acceptor spheres) and ρ_A is the density of acceptors. For comparison, a simple integration shows that the equation which governs the quenching by exchange interactions among a similar distribution of donors and acceptors has the form $k = 2\pi\rho_A k_0^{ex} e^{-2a/L}L(a^2 + aL + L^2/2)$. A similar form is obtained for the electron-transfer mechanism. These last two mechanisms are thus characterized by a steeper decline with distance than Förster transfer.

For the rapid-diffusion limit to prevail, the donor must have an excited-state lifetime in the millisecond or longer range (Thomas et al., 1978). Previous studies of energy transfer in the rapid-diffusion limit used the long-lived luminescence of Tb^{3+} to study a variety of systems. While useful, this approach is limited to cases where the Tb^{3+} can be bound specifically to a protein (to serve as donor to freely diffusing acceptors) or when the protein contains an acceptor chromophore (while Tb^{3+} is free to diffuse). Binding a donor or acceptor to the protein may result in structural changes in the protein which will affect the results of the measurement. Use of the intrinsic phosphorescence from tryptophan has the obvious advantages of not requiring chemical modifications and of being more generally applicable since tryptophan is an integral residue in almost all proteins. Under the appropriate conditions this emission can be very long lived (on the time scale of seconds) and hence quite appropriate for energy-transfer measurements in the rapid-diffusion limit. In most proteins only a small number of tryptophan residues (frequently one) significantly phosphoresce, making their identification easier and data interpretation more meaningful and applicable to the study of the protein. While energy transfer from a tryptophan triplet to a suitable acceptor at cryogenic temperature, i.e., in the static limit, has been reported (Galley & Stryer, 1969; Weers & Maki, 1986), the transfer at room temperature in the rapid-diffusion limit has not been utilized as yet.

The present study was undertaken with a number of objectives: (1) to demonstrate the applicability of energy transfer at the rapid-diffusion limit between phosphorescent tryptophan residues and suitable acceptors for the determination of the spatial distribution of phosphorescent tryptophans in proteins and (2) to identify and test useful models and experimental conditions for application of the technique. AP was chosen because it displays strong, long-lived, room-temperature phosphorescence in deoxygenated aqueous solutions. Three small dye molecules were selected which have similar structures but different spectral overlaps with AP. Likewise, the oxidized and reduced forms of Mb, as well as those of cytochrome c,

have similar structures and different spectral overlaps. This allows the measurement of the relative contribution of resonance energy transfer processes to the quenching while minimizing differences due to geometric considerations. The data show electron transfer from the triplet state of Trp to the dye molecules to be the dominant quenching mechanism. Electron transfer also dominates the quenching by met-Mb and by oxidized cytochrome *c* and occurs over a remarkable donor–acceptor separation. When the heme group is fully reduced (ferrous), the rate of quenching is strongly decreased and may be assumed to be solely due to resonance transfer at the rapid-diffusion limit. This allows the calculation of the distance of closest approach between the donor and acceptor, from which the distance of the phosphorescent Trp below the AP surface was calculated. The data show this residue to be embedded deep inside the protein.

Materials and Methods

Escherichia coli alkaline phosphatase (AP) type III-S was obtained from Sigma Chemical Co. as a crystalline suspension in 2.5 M ammonium sulfate solution. Horse skeletal muscle myoglobin (Mb) and horse heart cytochrome *c* were obtained from Sigma as lyophilized products and used without further purification. Methyl red (MR), methyl orange (MO), and 2-[(4-hydroxyphenyl)azo]benzoic acid (HABA) were also purchased from Sigma.

Solutions of AP for phosphorescence studies were prepared at a concentration of 0.5–1.0 mg/mL in 50 mM Tris·HCl buffer, pH. 7.5, containing 0.4% β-D-glucose. Samples of 500 μL of protein solution were placed in a quartz vacuum cuvette, and deoxygenation was initiated by covering the solution with a stream of ultrapure argon (<1 ppm O_2) which had been further extensively deoxygenated by passage through a solution of vanadyl sulfate as described by Englander et al. (1987). One microliter of a stock solution of 20 mg/mL glucose oxidase and 2 mg/mL catalase was then added and mixed into the sample with a magnetic stirrer. Ten minutes after the addition of these enzymes, O_2 levels were low enough to obtain AP phosphorescence lifetimes in excess of 1s. At this point the sample was overlayed with a layer of heavy mineral oil, which is an effective oxygen barrier. For maximal deoxygenation, 1 μL of a 20 mM solution of sodium dithionite, which acts as an oxygen scavenger, was then added.

Stock solutions of concentrated dye or of oxidized heme protein, to be used as energy acceptors, were deoxygenated in a manner identical with that of the sample. To generate the reduced heme proteins, the amount of dithionite added in the last deoxygenation step was slightly in excess of the amount required to reduce all of the heme groups. The completion of this reduction was monitored spectrophotometrically by the change in the absorption spectrum (Antonini & Brunori, 1971). To begin an experiment, the phosphorescence lifetime of the deoxygenated AP sample was measured. An appropriate amount of deoxygenated quencher solution was added, and the lifetime was remeasured. To ensure that quenching was due to the acceptor molecule and not O_2 contamination, aliquots of deoxygenated buffer were added in a separate experiment and shown not to decrease the sample lifetime.

The triplet state from which tryptophan phosphorescence occurs is populated from the first excited singlet state by intersystem crossing. The latter state was excited by a short pulse of laser radiation at 280 nm. Figure 1 illustrates the experimental configuration. The frequency-doubled pulses of a Spectra-Physics Model DCR-11 Nd:YAG laser were used with a wavelength of 532 nm and a duration of 8 ns (FWHM) to pump a Spectra-Physics Model PDL-3 dye laser emitting

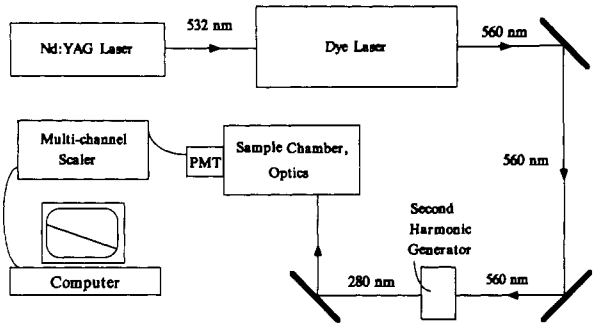

FIGURE 1: Block diagram of the equipment used to record phosphorescence decay kinetics. A more detailed description of the system is given under Materials and Methods.

at 560 nm, and this light was then focused into a second harmonic generating crystal to produce 280-nm radiation. The excess 560-nm light was removed by a Schott glass UG-11 filter, leaving only the ultraviolet light, which was directed into the sample.

The phosphorescence wavelength to be monitored was selected by an interference filter. The filter routinely used was centered at a wavelength of 450 nm with a FWHM of 25 nm. For samples with a high acceptor concentration (and consequently a high absorption at 450 nm), a stronger signal was often obtainable with filters centered at 500 or 550 nm. The phosphorescence lifetime was found to be identical at all these wavelengths. The phosphorescence signal was detected by a Hamamatsu R928P photomultiplier tube, especially selected for low dark current and set up for photon counting. The tube was operated at −20 °C to further minimize dark counts. The impinging of tryptophan fluorescence on the PMT was eliminated by a mechanical shutter which opened 2 ms after each laser flash. Pulses from the photomultiplier tube were sent into a Pacific Instruments Model AD6 amplifier/discriminator, whose output was collected by an ACEMCS multichannel scaler from EG&G Ortec, capable of collecting counts at up to 100 MHz. The calibration of the scaler was checked by sending in pulses at 10 Hz and measuring the spacing of peaks detected. The equipment described is capable of collecting decay curves over six to seven lifetimes for each excitation pulse. This facilitates data collection and reduces the chances of damaging the sample with an excessive number of laser pulses. The low noise in the system allows reliable measurements of the small changes in lifetime even during detection of weak phosphorescence signals. Analysis of the phosphorescence decay curves was performed with computer software which applied a Marquadt χ^2 algorithm (Bevington, 1969). It is worthwhile to note that the short duration of the excitation pulse relative to the phosphorescence decay makes deconvolution of the data unnecessary.

Steady-state phosphorescence spectra were measured on a SPEX Industries Model DM1B fluorometer equipped with phosphorimeter Module 1934C. The excitation was from a 150-W xenon flash lamp, centered at 280 nm and with a bandwidth of 18 nm. Emission was recorded with a resolution of 2.7 nm, with a delay of 0.1 ms after the firing of the lamp. Absorption spectra were recorded on a Shimadzu Model UV-260 spectrophotometer with a bandwidth of 5 nm.

The radiative efficiency of the triplet state ϕ_p, which is relevant for triplet–singlet energy transfer, is the ratio between the number of phosphorescence photons emitted and the number of molecules excited to the triplet state. Thus, $\phi_p = \tau_o/\tau_R$, where τ_o is the observed phosphorescence lifetime in the absence of quencher and τ_R is the radiative lifetime of the phosphorescence. For the latter, we used a value of 11.5 s,

Table I: Comparison of Parameters Used in Distance Calculations between AP Donor and Various Acceptors

acceptor	$J \times 10^{14}$ (M^{-1} cm^3)	av R_0 (Å)	$k_0R_0^6$ ($Å^6$ s^{-1})	k_t (mM^{-1} s^{-1})
MR	6.4	34.4	1.04×10^9	20.9
MO	7.7	35.4	1.26×10^9	18.1
HABA	0.7	23.6	1.11×10^8	23.0
met-Mb	9.2	36.8	1.50×10^9	0.30
Mb	12.3	39.6	2.01×10^9	0.07
oxidized cyt *c*	7.0	34.7	1.14×10^9	0.35
reduced cyt *c*	7.3	35.6	1.19×10^9	0.10

based on the values of the lifetime and quantum yield of chymotrypsin phosphorescence (Galley & Stryer, 1969) and assuming the radiative decay time of the AP tryptophan phosphorescence to be the same as that of chymotrypsin. We routinely obtained a lifetime of 1.9 s for AP, giving a radiative efficiency of $\phi_p = 1.9/11.5 = 0.17$. τ_0, the phosphorescence lifetime in absence of quencher, was however found to vary somewhat among different experiments (possibly due to variations in the efficiency of oxygen removal). It is important to note that while this variability in lifetime affects the values derived for R_0^6, the measured parameter k_t in fact depends on $k_0R_0^6$ (see eq 1). This quantity can be rewritten as R_0^6/τ_0, and since R_0^6 is proportional to τ_0 (through ϕ_p), the lifetime fluctuations will not affect the quenching rate constant k_t.

Results

The steady-state room-temperature phosphorescence spectrum of AP is depicted in Figure 2A along with the structures and absorption spectra of MR, MO, and HABA, which served as phosphorescence quenchers.

Figure 2B illustrates the overlap of the emission spectrum of AP with the absorption spectra of Mb and met-Mb, while Figure 2C shows the corresponding spectra for reduced and oxidized cytochrome *c*. The data presented in Figure 2 were used to calculate the overlap integrals *J*, and the corresponding values are given in Table I. The table also lists the values of R_0 for each of these AP–acceptor pairs, calculated from the respective spectral overlaps, by use of a value of 2/3 for K^2 and by determination of the radiative efficiency of the triplet state from the ratio between the observed and radiative lifetimes, as described under Materials and Methods.

Typical phosphorescence decay curves of AP in the absence of energy acceptors as well as in the presence of 1 mM met-Mb are shown in Figure 3A while Figure 3B depicts the effects of the dye MO on the decay rate of the triplet state. The molar quenching rate constants k_t/C_A (where C_A is the acceptor concentration) as derived from the data are also given in Table I. As indicated by the linear dependence of the logarithm of phosphorescence intensity on time (see Figure 3) and corroborated by data analysis, all the phosphorescence decay curves obtained in the present study are well fit by monoexponential decay laws. The observation that tryptophan phosphorescence, unlike fluorescence, decays monoexponentially is in agreement with previous reports based on data obtained in glassy matrices at cryogenic temperatures (Strambini & Gonnelli, 1985) and for proteins in fluid solution (Vanderkooi et al., 1987). The monoexponential decays observed in the presence of acceptor molecules (shown in Figure 3) support the view that the quenching of the phosphorescence is not due to (static) binding of acceptor molecules to the protein being studied. If this were the case, one would expect contributions from free and bound protein molecules to be present in the phosphorescence, yielding biexponential decays whose amplitudes would depend on the concentration of acceptor. The linear dependence of the quenching rate constant on acceptor concentration (see Figure 4) also shows the quenching to be a dynamic process.

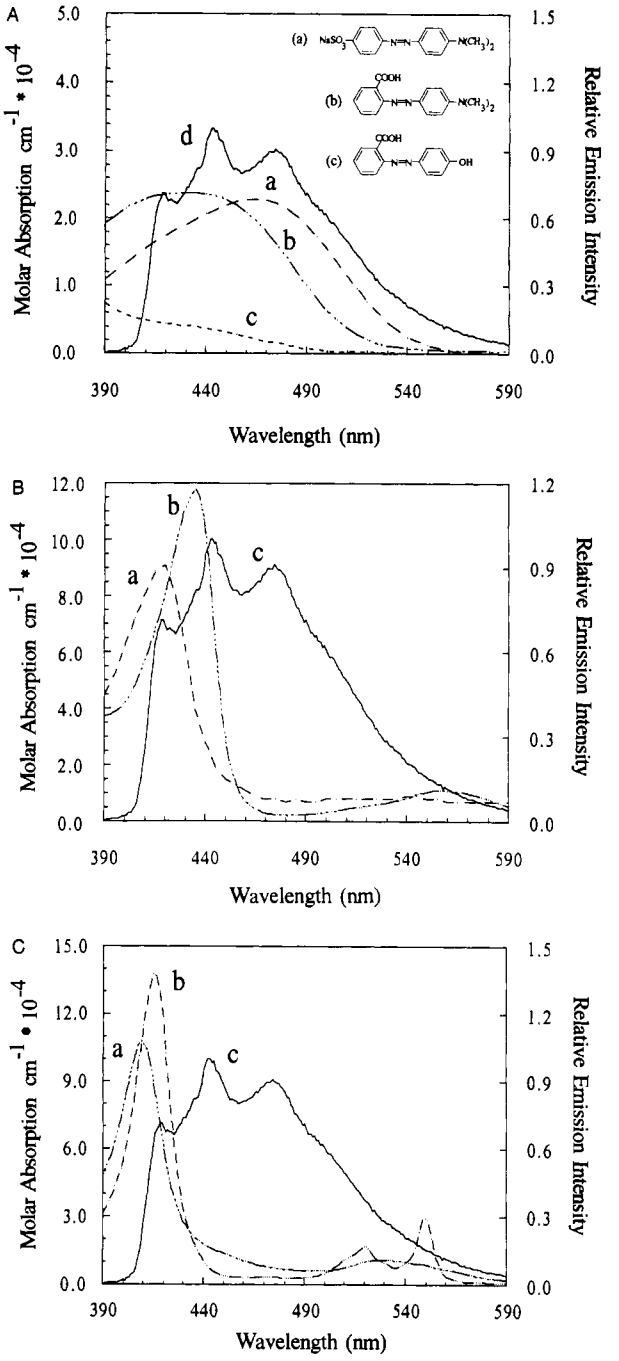

FIGURE 2: (A) Molar absorption spectra of the dyes used to quench AP phosphorescence: (a) methyl orange, (b) methyl red, and (c) HABA. The corresponding structures are depicted in the inset. (d) the normalized steady-state phosphorescence spectrum of AP in a deoxygenated aqueous solution at room temperature, excited at 287 nm with a bandwidth of 18 nm. The emission was recorded following a delay time of 0.1 ms with a spectral bandwidth of 3.6 nm. (B) Molar absorption spectrum of (a) met-Mb and of (b) deoxy-Mb. The phosphorescence emission spectrum of AP at room temperature is also depicted in (c). (C) Molar absorption spectra of (a) oxidized cytochrome *c* and of (b) reduced cytochrome *c*. The phosphorescence emission spectrum of AP at room temperature is also shown in (c).

Table I summarizes the quenching rate constants found for each of the acceptor molecules. HABA was found to quench AP phosphorescence more effectively than either MR or MO, in spite of the fact that its spectral overlap integral with AP is only $^1/_{10}$ that of the other two dyes. The lack of dependence of quenching rate on the overlap of the spectra indicates that

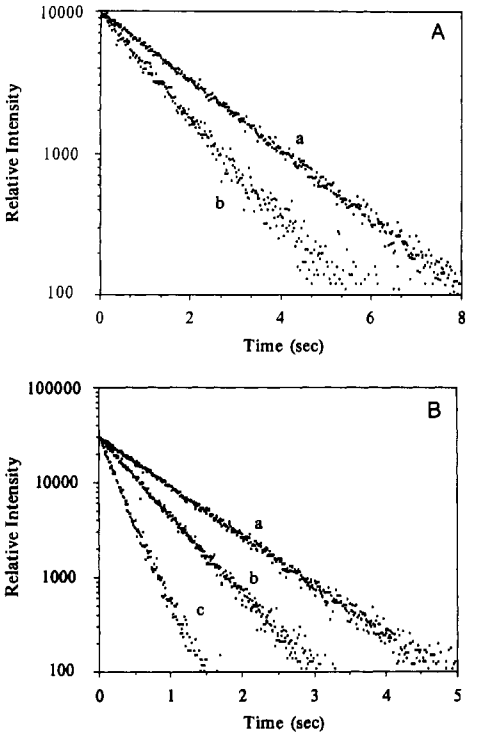

FIGURE 3: (A) Effect of met-Mb on the phosphorescence decay of AP: (a) decay of emission of AP with no met-Mb present, with τ = 1.77 s; (b) decay of AP emission in the presence of 1.0 mM met-Mb, with τ = 1.17 s. (B) Effect of MO on the phosphorescence decay of AP: (a) decay of AP in the presence of 10 μM MO, with τ = 0.82 s; (b) decay of AP in the presence of 50 μM MO, with τ = 0.52 s; (c) decay of AP in the presence of 200 μM MO, with τ = 0.24 s.

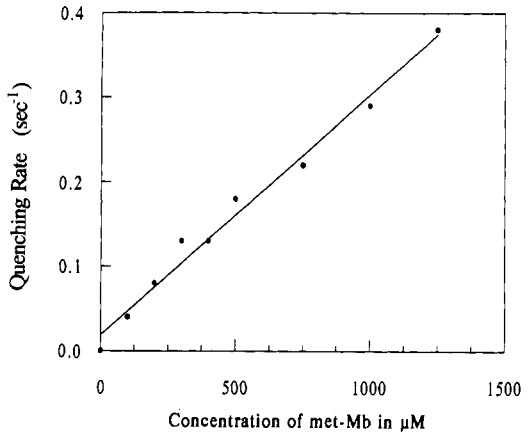

FIGURE 4: Dependence of the quenching rate of AP phosphorescence on met-Mb concentration. This was calculated from $1/\tau - 1/\tau_0$ for the rate, where τ_0 and τ are the lifetimes in the absence and presence of a given quencher concentration.

resonance processes (Förster transfer and the exchange mechanism) make at most only a small contribution to the quenching. When a small excess of sodium dithionite was added to the sample so as to fully reduce the dye, the AP lifetime returned to its value in absence of dye, in support of electron transfer as the main quenching mechanism, since the reduced dye is a poor electron acceptor. The lack of residual quenching from resonance transfer processes is due to the fact that the dithionite also bleaches the dyes, and hence, the value of the spectral overlap becomes zero. A lack of dependence of quenching rate on spectral overlap also characterizes the quenching of AP phosphorescence by the heme proteins. For both Mb and cytochrome *c*, the overlap integral of the reduced heme is slightly larger than that of the oxidized heme (5% larger for cytochrome *c*; 33% larger for Mb), yet in both cases

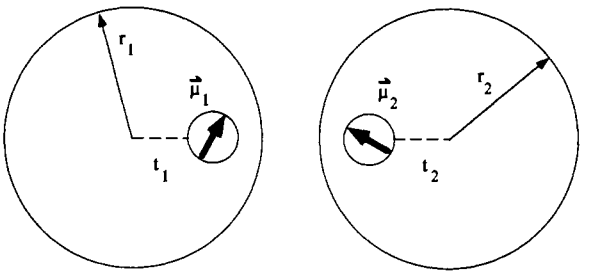

FIGURE 5: Geometry of the model used for quenching of AP phosphorescence by the heme proteins. Both AP and the heme proteins are assumed to be spheres with radii r_1 and r_2 while both the heme group and the phosphorescent tryptophan are taken to be off center at distances t_1 and t_2. μ_1 and μ_2 are the transition dipole moment vectors of each chromophore, here assigned an arbitrary fixed orientation relative to their respective proteins; however in order to set $K^2 = 2/3$, these vectors must be allowed to assume all orientations (see text).

the oxidized form of the protein has a quenching constant several times larger than that of the reduced form. This observation indicates that quenching by the oxidized heme proteins is dominated by electron transfer. Electron transfer is eliminated when the heme group is reduced and becomes a poor electron acceptor, as evidenced by the fact that it cannot be further reduced by dithionite. It is therefore reasonable to assume that the quenching of AP phosphorescence by the reduced-heme proteins is solely due to energy exchange and Förster transfer. Since the rate of these transfer mechanisms is proportional to the spectral overlap, the contribution of resonance energy transfer to the rate constant for quenching by the oxidized heme group is easily found from the transfer rate to the reduced heme group by scaling to account for the difference in the overlap integrals. Such a calculation shows that for met-Mb the overall quenching rate consists of k_t = 0.25 mM^{-1} s^{-1} for electron transfer and of k_t = 0.05 mM^{-1} s^{-1} for resonance energy transfer. A similar calculation for oxidized cytochrome *c* yields the values of k_t = 0.25 mM^{-1} s^{-1} for electron transfer and k_t = 0.10 mM^{-1} s^{-1} for resonance transfer mechanisms.

If the resonance transfer rates evaluated above are assumed to be due to Förster transfer alone, then they may be used to determine the distance of closest approach between the heme group and the phosphorescent Trp, from which the distance from this tryptophan to the AP surface may be evaluated. The contribution of exchange interactions is thus being ignored, an assumption which will have to be reconsidered if the distances of closest approach determined turn out to be within the range of this interaction, about 10–15 Å. The calculated distance depends on the geometry of the model used to represent the molecules involved. In our calculation the interacting molecules were assumed to be uncharged spheres with radii r_1 and r_2, with the chromophores participating in the transfer situated off center at distances t_1 and t_2, as depicted in Figure 5. We have recently derived the expression for the quenching rate constant in this case to be

$$k_t = \frac{4\pi}{3}\rho_A k_o R_o^6 \frac{(a + t_1 + t_2)^3(a^2 + 2at_1 + 2at_2 + 2t_1t_2)}{a^2(a + 2t_1)^2(a + 2t_2)^2(a + 2t_1 + 2t_2)^2} \quad (3)$$

assuming a value of $^2/_3$ for K^2. Here $a = r_1 + r_2 - t_1 - t_2$. This derivation thus assumes that at each donor–acceptor separation a complete averaging over all angles between the dipole moments and between each of the dipoles and the vector connecting them is possible. This assumption is strictly valid only for a spherically symmetric geometry and does not apply to an off-center chromophore whose dipole moment orientation

is fixed with respect to the protein in which it is embedded (see Discussion). When these chromophores are not close to the surface of the spheres, however, it can be shown that the error generated by assuming $K^2 = {}^2/_3$ is not large (Mersol et al., unpublished results).

In order to use eq 3 to evaluate the depth of the phosphorescent tryptophan beneath the surface of AP, values for the radii of both donor (AP) and acceptor (Mb or cytochrome *c*) as well as the offset distance from the center of each heme protein to the center of the heme must be assigned. The radii of Mb and cytochrome *c* were determined by finding the radius of a sphere with the same volume as each protein. These volumes were determined from the specific volumes $\bar{V}$ and the molecular weights of each, by use of the equation $V = M\bar{V}/N$, where N is Avogadro's number. The values of specific volume of 0.72 mL/g for cytochrome *c* and 0.74 mL/g for Mb (Kuntz & Kauzmann, 1974) along with molecular weights of 12400 for cytochrome *c* (Sigma Chemical Co.) and 18000 for Mb (Antonini & Brunori, 1971) yield equivalent radii of 15.2 Å for cytochrome *c* and 17.4 Å for Mb. The offset distance of the heme group in cytochrome *c* was obtained by positioning the iron so that the outer edge of the porphyrin ring lies at the surface of the protein, since this edge is known to be exposed to the surface (Koppenol & Margoliash, 1981). The offset distance obtained in this manner is 9.7 Å. The offset distance of the heme group in Mb was taken as the distance from the center of volume of the Brookhaven X-ray coordinates for sperm whale myoglobin to the iron atom of the heme group. In Mb, the center of the heme group is thus 7.8 Å from the protein center. The value used for the radius of AP was 30 Å (Reid & Wilson, 1970). When these values are inserted into eq 3 along with the measured quenching rates for the reduced heme proteins, the quenching by Mb predicts a Trp offset distance of 14 Å while that by cytochrome *c* predicts an offset distance of 22 Å. These translate into a depth beneath the AP surface of 16 Å from the Mb quenching and 8 Å from that due to cytochrome *c*. The closest approach distance between the Mb heme and AP Trp is outside the range of the exchange interaction, and so the assignment of the resonance transfer rate solely to Förster transfer is supported for this pair. Cytochrome *c*, with its heme closer to the surface yields a smaller closest approach distance which lies at the edge of the range for exchange interactions, and thus its AP quenching rate may include a contribution from this mechanism.

Equations 2 and 3 were developed by assuming a homogeneous distribution of acceptors around each donor and thus neglect any electrostatic repulsion or attraction between donor and acceptor which might skew this distribution. Theoretical treatments of this effect have been developed (Wensel & Meares, 1983; Van Leeuwen, 1983). The distribution of electrostatic charges on cytochrome *c* can play an important role in the interactions of this protein with other proteins around it (Koppenol & Margoliash, 1981). To test for the presence of these effects in the phosphorescence quenching rates, the quenching of AP by Mb was compared at pH 7.5 and at pH 8.7, above and below the p*I* of Mb, thereby effectively placing opposite charges on Mb in the two experiments. No significant difference in quenching rate was seen in the two cases, and electrostatic attraction does not seem to play a role here. As the p*I* of cytochrome *c* is 10.6 (Lehninger, 1975) and that of AP is 4.5 (Reid & Wilson, 1970), it was not practical to apply the same method here due to possible changes in protein conformation at extreme pH values. The pH used in the phosphorescence quenching experiments was 7.5, placing opposite net charges on the two proteins. This results in electrostatic attraction and hence in an increased quenching rate relative to the rate in the absence of such attraction, due to the increased density of acceptors around the donor. High salt concentration screens electrostatic charges, which weakens the attractive force and would be expected to cause a decrease in quenching (Lyle & Meares, 1983). In order to mask any possible electrostatic effects in the transfer to cytochrome *c*, the AP quenching by this acceptor was also determined in the presence of 1 M concentrations of Tris·HCl or $MgSO_4$, both at pH 7.5. The addition of the $MgSO_4$ did not appreciably alter the quenching rate. However, the addition of high concentrations of Tris-HCl did result in a significant decrease in quenching rate by approximately 30%, down to 0.07 mM^{-1} s^{-1}. This translates into a distance below the surface of 12 Å for the phosphorescent Trp, in closer agreement with the Mb data, and suggests that the possibility of enhanced quenching of AP phosphorescence by cytochrome *c* due to electrostatic attraction cannot be ruled out.

The difference in the values obtained for the depth of the emissive Trp below the surface of AP from the Mb and cytochrome *c* data is at least partially due to the fact that the structures of these proteins differ from the simplistic model of Figure 5. More realistic representations of these molecules which account for the deviations of the proteins from uncharged spheres may be expected to yield better values for the distances of closest approach and, in turn, for the depth of the phosphorescent tryptophan from the protein surface. Figures presented by Sowadski et al. (1985) based on X-ray crystallography show that Trp 109 lies 15–20 Å beneath the AP surface, while the other two Trps (Trp 220 and Trp 268) are at the protein surface. The value of 16 Å obtained from the Mb data for the depth beneath the AP surface agrees well with the actual depth of Trp 109, indicating that the AP–Mb interaction is fairly well represented by the geometry of Figure 5. The data from cytochrome *c* yield a distance of closest approach which is unrealistically small, reflecting the need for a model for this protein which better describes its shape and electrostatic interactions.

Discussion

The long decay times of protein phosphorescence in extensively deoxygenated aqueous solutions make the emitting tryptophan residues ideal energy donors to be used in diffusion-enhanced resonance energy transfer measurements. The distance of these residues from the surface of proteins as evaluated by this technique may be used to follow conformational changes that occur upon binding and dissociation of substrates and coenzymes, to monitor subunit association–dissociation and unfolding, and to observe protein–protein or protein–membrane interactions. In this respect tryptophan phosphorescence has an advantage over the use of extrinsic long-lived luminescent probes, like Tb^{3+}, which have been employed in several previous studies (Stryer, 1982). However, quenching by mechanisms other than resonance transfer also occurs and makes this approach more involved. Indeed, the quenching of the phosphorescence of several proteins by small molecules (O_2, CO, H_2S, CS_2) showed little sensitivity to the nature of the protein and suggested that these small quenchers penetrate into the protein to interact directly with the phosphorescent tryptophan residue (Calhoun et al., 1988). Larger quenchers (ethanethiol, methyl vinyl ketone, etc.) were found not to penetrate into rigid sites of phosphorescent tryptophans and also not to quench by colliding with tryptophan residues temporarily exposed to the aqueous solution (as would occur

during protein-opening reactions in fluctuating protein molecules). The results were interpreted as suggesting a quenching mechanism that involves long-range interactions between the quencher and the buried tryptophan. Since the absorption spectra of the quenchers used in the studies cited above do not overlap tryptophan phosphorescence, Förster-type energy transfer is not a valid mechanism for the observed quenching, and it was concluded that the luminescence was quenched by an electron-transfer mechanism (Calhoun et al., 1988). The rate of electron transfer decays steeply with the donor–acceptor distance, declining by as much as a factor of 7 for each additional angstrom of separation (Marcus & Sutin, 1985). This mechanism was thus suggested to be most effective over distances smaller than 10–12 Å (Turro, 1978). The relatively long lifetime of tryptophan phosphorescence in many proteins may compensate for a smaller rate constant and hence allow electron transfer to be an effective triplet-state quencher over significantly larger distances. Unlike dipole–dipole energy transfer, electron-transfer reaction rates also critically depend on the nature of the medium separating the electron donor and acceptor. The application of these transfer rates to distance determination is hence not a straightforward procedure, although progress in this area has recently been reported (Vanderkooi et al., 1990).

In the present study the rates of quenching of the room-temperature phosphorescence of AP in solution by two heme proteins and by several small dye molecules were determined. The phosphorescence quenching rate of AP by the small dye molecules was found to be independent of the overlap of the emission and absorption spectra. This observation demonstrates that mechanisms other than dipole–dipole transfer or energy exchange dominate the transfer. Since the dyes employed in the present study are larger than the quenchers used by Calhoun et al. (1988), their penetration into the protein to collide with the excited tryptophan residue is unlikely and cannot explain our data. Reduction of these dyes by a small excess of dithionite removed the quenching, and this is attributed mostly to a reduction in the electron-accepting potential of the reduced dyes and not to a change in the overlap integral, as this quantity was already found not to affect the quenching rate. We thus conclude that long-range electron transfer is predominantly responsible for the quenching by nonreduced quenchers.

It should be noted that the AP molecule has a large active site pocket into which small dye molecules can fit and thus approach interior tryptophans. Trp 109, which is thought to be the phosphorescent residue in AP (Strambini, 1987), is closer to this pocket than to the outer surface of AP, as evidenced by the presence of an H_2O molecule only 7.5 Å from the indole nitrogen in the X-ray-determined structure (H. Wyckoff, personal communication). Since the rate of electron transfer (the presumed quenching mechanism in this case) strongly depends on donor–acceptor separation, such penetration of the dye molecules into the active site of AP may explain why these molecules are approximately 100-fold more efficient at quenching AP phosphorescence than Mb and cytochrome *c*, which are obviously too large to enter the active site pocket.

The assumption that the quenching of AP phosphorescence by the reduced heme proteins proceeds solely by Förster transfer allows the calculation of the distance of closest approach between donor and acceptor, from which the depth of the emitting Trp beneath the surface of the AP can be evaluated. Using eq 3 and the AP-Mb data yields a value 16 Å between the phosphorescent Trp and the AP surface, while the data for cytochrome *c* in dilute buffer predict a depth of 8 Å. The quenching of AP by Mb was not affected upon reversal of the net charge of Mb by increasing the pH of the buffer to a value above its p*I*, demonstrating that electrostatic effects are not altering the transfer rate. The depth of 16 Å is close to the distance from the AP surface to Trp 109, while the other two Trps lie near the protein surface. We thus assign the phosphorescence of AP to Trp 109, in agreement with previous reports (Saviotti & Galley, 1974; Strambini, 1987).

The smaller distance from the phosphorescent Trp to the AP surface calculated from the quenching by cytochrome *c* may be an indication that attractive electrostatic forces are significantly affecting the transfer by inducing a greater local concentration of acceptors around each donor. In 1 M Tris·HCl the transfer rate from AP to cytochrome *c* was indeed found to decrease by 30% to 0.07 mM^{-1} s^{-1}. If this lower value is taken to be the undistorted transfer rate, a minimum distance from the AP surface to the phosphorescent Trp of 12 Å is obtained, which is in better agreement with the distance obtained from the Mb data. While electrostatic interactions may play an important role, other factors, most notably the molecular shape, can also strongly affect the rate of energy transfer. AP, Mb, and cytochrome *c* are better described as ellipsoids than as spheres, and the extent to which their shapes differ from a sphere will affect their respective quenching rates. A chromophore embedded inside an ellipsoid will exhibit an enhanced transfer rate relative to one which is embedded in a sphere of the same volume, since the increased quenching from acceptors being able to approach closer along the minor axis of the ellipsoid will more than compensate for the decreased quenching along the major axis, as the $1/r^6$ dependence of the interaction heavily weights contributions to the transfer from closer distances. The rate of transfer from AP is also affected by the orientation of the dipole of the heme group, which is different in cytochrome *c* and Mb. As stated under Results, eqs 2 and 3 assume complete randomization of the angle of the dipoles with respect to each other and of the angle each dipole makes with the vector joining them, an assumption which is not valid for geometries which lack spherical symmetry and whose transition dipoles retain a fixed orientation with respect to the embedding molecules. Although the phosphorescence lifetime of AP is orders of magnitude longer than the rotational relaxation time of the protein, complete averaging of the angles in the geometry of Figure 5 (with fixed orientation of the dipoles relative to their respective proteins) is prevented by steric hindrance of one protein by the other for all dipole–dipole separations which are less than $r_1 + r_2 + t_1 + t_2$. Thus in deriving the expression for the quenching rate from eq 1 for the geometry of Figure 5, orientation and distance are not independent at small donor–acceptor separations, and K^2 cannot be assigned a fixed average value. It can be shown, however, that for chromophores which are not near the surface of the protein the error obtained by setting $K^2 = 2/3$ (which assumes that the orientation of each dipole with respect to its embedding protein is not fixed) will be no more than a few percent.

The deviations from the ideal behavior in eq 3 described above will have a more pronounced effect on the quenching rate for chromophores which are nearer to the surface. Since the dipole–dipole interaction scales as $1/r^6$, a chromophore which is closer to nonspherical areas of the protein surface, for example, will be more affected by surface curvature than one which is deeply buried beneath the surface. The enhanced quenching rate of AP by cytochrome *c* may therefore also reflect the fact that the heme group in cytochrome *c* touches

the protein surface, making its nonspherical shape and the incomplete angle averaging much more important factors for increasing the quenching rate than those of Mb with its buried heme.

It is clear that improved models which give more realistic approximations to protein structure will yield better distance measurements and will allow for the use of a wider range of probes. Equation 3 in this paper, which describes the quenching in a situation in which both chromophores are off center (assuming complete angular averaging), already shows a substantial improvement over the previously known formulas. This equation is of course applicable to donors other than tryptophan and should also extend the usefulness of extrinsic, bound probes to protein distance measurements. We are currently developing equations which will properly account for the averaging of the dipole angles, as well as ones which will allow for ellipsoidal shapes to be used for the molecules. Nevertheless, the fact that even the current, simple model yields values which are close to the actual depth of Trp 109 in AP shows that with the right choice of probe the technique of diffusion-enhanced phosphorescence energy transfer can be useful for distance measurements in protein structure studies. The fact that the tryptophan triplet state is also an effective donor of electrons limits the choice of energy acceptors to species which are poor electron acceptors (or at least those whose electron-transfer rate can be separately measured). When such an acceptor has been found and contributions from the exchange interactions accounted for, the Förster transfer equations may be applied. Although the embedded heme group of Mb fits these criteria, it would also be useful to find a smaller probe whose Förster transfer rate can be determined.

Registry No. MR, 493-52-7; MO, 547-58-0; HABA, 1634-82-8; AP, 9001-78-9; L-Trp, 73-22-3; cytochrome *c*, 9007-43-6.

References

Antonini, E., & Brunori, M. (1971) *Hemoglobin and Myoglobin in Their Reactions with Ligands*, American Elsevier Publishing Co., New York.

Bevington, P. R. (1969) *Data Reduction and Error Analysis for the Physical Sciences*, McGraw-Hill, New York.

Calhoun, D. B., Englander, S. W., Wright, W. W., & Vanderkooi, J. M. (1988) *Biochemistry 27*, 8466.

Englander, S. W., Calhoun, D. B., & Englander, J. J. (1987) *Anal. Biochem. 161*, 300.

Förster, Th. (1948) *Ann. Phys. 2*, 55.

Förster, Th. (1949) *Z. Naturforsch., A 4*, 321.

Galley, W. C., & Stryer, L. (1969) *Biochemistry 8*, 1831.

Ghiron, C., Bazin, M., & Santus, R. (1988) *Biochim. Biophys. Acta 957*, 207.

Gösele, U. (1978) *Spectrosc. Lett. 11*, 445.

Gösele, U., Hauser, M., Klein, U. K. A., & Frey, R. (1975) *Chem. Phys. Lett. 34*, 519.

Kai, Y., & Imakubo, K. (1979) *Photochem. Photobiol. 29*, 261.

Klein, U. K. A., Frey, R., Hauser, M., & Gösele, U. (1976) *Chem. Phys. Lett. 41*, 139.

Koppenol. W. H., & Margoliash, E. (1981) *J. Biol. Chem. 257*, 4426.

Kuntz, I. D., Jr., & Kauzman, W. (1974) *Adv. Protein Chem. 28*, 239.

Lehninger, A. (1975) *Biochemistry*, Worth Publishers, New York.

Li, Z., Lee, W. E., & Galley, W. C. (1989) *Biophys. J. 56*, 361.

Marcus, R. A., & Sutin, N. (1985) *Biochim. Biophys. Acta 811*, 265.

Mayo, S. L., Ellis, W. R., Jr., Crutchley, R. J., & Gray, H. B. (1986) *Science 23*, 948.

Millar, D. P., Robbins, R. J., & Zewail, A. H. (1981) *J. Chem. Phys. 75*, 3649.

Papp, S., & Vanderkooi, J. M. (1989) *Photochem. Photobiol. 49*, 75.

Phillips, S. E. V. (1980) *J. Mol. Biol. 142*, 531.

Reid, T. W., & Wilson, I. B. (1970) in *The Enzymes* (Boyer, P. D., Ed.) Vol. IV, p 373, Academic Press, New York.

Saviotti, M. L., & Galley, W. C. (1974) *Proc. Natl. Acad. Sci. U.S.A. 71*, 4154.

Sowadski, J. M., Handschumacher, M. D., Krishna Murthy, H. M., Foster, B. A., & Wyckoff, H. W. (1985) *J. Mol. Biol. 186*, 417.

Steinberg, I. Z., & Katchalski, E. (1968) *J. Chem. Phys. 48*, 2404.

Steinberg, I. Z., Haas, E., & Katchalski-Katzir, E. (1983) in *Time Resolved Fluorescence Spectroscopy in Biochemistry and Biology* (Cundall, R. B., & Dale, R. E., Eds.) pp 411–450, Plenum Press, New York.

Strambini, G. B. (1987) *Biophys. J. 52*, 23.

Strambini, G. B., & Gonnelli, M. (1985) *Chem. Phys. Lett. 115*, 196.

Stryer, L. (1978) *Annu. Rev. Biochem. 47*, 819.

Stryer, L., Thomas, D. D., & Meares, C. F. (1982) *Annu. Rev. Biophys. Bioeng. 11*, 203.

Thomas, D. D., Carlsen, W. F., & Stryer, L. (1978) *Proc. Natl. Acad. Sci. U.S.A. 75*, 5746.

Turro, N. J. (1978) in *Modern Molecular Photochemistry*, pp 305–309, Benjamin Cummings Publishing Co., Menlo Park, CA.

Vanderkooi, J. M., Calhoun, D. B., & Englander, S. W. (1987) *Science 236*, 568.

Vanderkooi, J. M., Englander, S. W., Papp, S., Wright, W. W., & Owen, C. S. (1990) *Proc. Natl. Acad. Sci. U.S.A. 87*, 5099.

Van Leeuwen, J. W. (1983) *Biochim. Biophys. Acta 743*, 408.

Weers, J. G., & Maki, A. H. (1986) *Biochemistry 25*, 2897.

Wensel, T. G., & Meares, C. F. (1983) *Biochemistry 22*, 6247.